DOI: 10.1002/ejic.200500904

Syntheses, Structures and Characterisation of Two Cu^{II} Polymers with 8-Connected Topologies Based on Highly Connected SBUs

Jian Zhang,[a] Yao Kang,[a] Jie Zhang,[a] Zhao-Ji Li,[a] Ye-Yan Qin,[a] and Yuan-Gen Yao*[a]

Keywords: Coordination polymers / Copper / Hydrothermal synthesis / Magnetic properties / N ligands

Two hydrothermally synthesised 3D metal-coordination polymers, namely [Cu(isonicotinate)(nicotinate)]$_n$ (**1**), with an 8-connected CsCl topology, and [Cu_2(μ_3-OH)(isonicotinate)$_2$-(BDC)$_{0.5}$]$_n$ (**2**), with an unusual 8-connected $3^5.4^{11}.5^8.6^4$ topology, demonstrate that highly connected SBUs can be employed in the construction of complicated frameworks. The temperature-dependent magnetic susceptibilities for the two complexes were also determined.

Introduction

Recent studies on inorganic/organic hybrid materials, especially in the area of metal–ligand coordination framework polymers, have enriched crystal engineering and have provided a wide range of inorganic networks in the solid state.[1] A large number of the lowly connected network topologies depicted by Wells[2] are commonly found in framework materials such as zeolites and in coordination polymers.[3] However, highly connected topologies are still a major challenge to chemists because the construction of such systems is severely hampered by the available number of coordination sites at the metal centres and the steric demand of the organic ligands. Yaghi et al. have developed a SBU (secondary building unit) strategy to direct the assembly of metal–organic frameworks (MOFs), which has been widely used for understanding and predicting structural topologies.[4] Most recently, Champness et al. have successfully obtained a series of highly connected topologies by selecting high coordinate lanthanide metals and flexible 4,4′-bipyridine-*N*,*N*′-dioxide ligands.[5] Although a large number of crystalline materials constructed from SBUs and linkers have been reported, the construction of highly connected topologies based on highly connected SBUs are extremely rare.[6] Compared with complexes with d- or f-block metal nodes, complexes with metal cluster nodes generally have weak metal–metal interactions and some interesting physical properties, such as luminescence and magnetism. We report here two novel polymers, namely [Cu(isonicotinate)(nicotinate)]$_n$ (**1**) and [Cu_2(μ_3-OH)(isonicotinate)$_2$(BDC)$_{0.5}$]$_n$ (**2**; BDC = 1,3-benzenedicarboxylate), which exhibit 8-connected CsCl and non-CsCl topologies, respectively.

[a] State Key Laboratory of Structural Chemistry, Fujian Institute of Research on the Structure of Matter, The Chinese Academy of Sciences,
Fuzhou, Fujian 350002, China
Fax: +86-591-8371-4946
E-mail: yyg@ms.fjirsm.ac.cn

Results and Discussion

X-ray Crystal Structure of [Cu(isonicotinate)(nicotinate)]$_n$ (1)

The single-crystal X-ray structure of complex **1** reveals that it adopts a 3D structure consisting of dimetallic clusters bridged by both nicotinate and isonicotinate ligands. Each Cu^{II} cation exhibits a distorted trigonal-bipyramidal geometry with an N_2O_3 coordination sphere from three nicotinate ligands and two isonicotinate ligands (Figure 1 and Table 1). Nicotinate acts as a μ_3-ligand with its carboxylate group bridging two Cu atoms that are separated by 4.330 Å. As shown in Figure 2 (a), the nicotinate ligands bridge the dinuclear copper clusters to form a 2D sheet parallel to the *bc* plane. The isonicotinate ligand bridges the Cu centres through one O donor and one N donor to form a zigzag chain in a head-to-tail manner. These chains are also linked by the carboxylate group of nicotinate ligands to form another 2D sheet almost parallel to the *ab* plane (Figure 2, b). In other words, each dinuclear copper cluster binds to four nicotinate ligands and four isonicotinate ligands simultaneously.

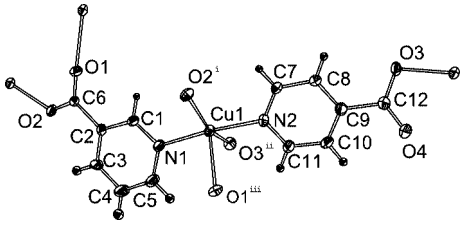

Figure 1. An ORTEP drawing of the molecular structure of complex **1**. For definition of i, ii and iii see footnote a in Table 1.

Table 1. Selected bond lengths [Å] and angles [°] for **1** and **2**.

Complex **1**[a]			
Cu1–O2^{i}	1.955(4)	Cu1–N2	2.037(5)
Cu1–O3^{ii}	1.999(4)	Cu1–O1^{iii}	2.248(5)
Cu1–N1	2.031(5)		
O2^{i}–Cu1–O3^{ii}	152.4(2)	N1–Cu1–N2	174.2(2)
O2^{i}–Cu1–N1	91.1(2)	O2^{i}–Cu1–O1^{iii}	115.24(18)
O3^{ii}–Cu1–N1	89.3(2)	O3^{ii}–Cu1–O1^{iii}	92.34(18)
O2^{i}–Cu1–N2	94.5(2)	N1–Cu1–O1^{iii}	86.9(2)
O3^{ii}–Cu1–N2	86.4(2)	N2–Cu1–O1^{iii}	89.4(2)
Complex **2**[b]			
Cu1–O3^{i}	1.9687(14)	Cu2–O6^{iii}	1.9062(14)
Cu1–O7	2.0015(14)	Cu2–O7^{iii}	1.9659(14)
Cu1–N2^{ii}	2.0045(17)	Cu2–O7	1.9702(15)
Cu1–O1	2.0431(14)	Cu2–N1	1.9828(16)
Cu1–O5	2.1844(15)	Cu2–Cu2^{iii}	3.0057(6)
O3^{i}–Cu1–O7	91.78(6)	N2^{ii}–Cu1–O5	88.79(6)
O3^{i}–Cu1–N2^{ii}	91.38(6)	O1–Cu1–O5	100.61(6)
O7–Cu1–N2^{ii}	176.31(6)	O6^{iii}–Cu2–O7^{iii}	94.14(6)
O3^{i}–Cu1–O1	157.30(6)	O6^{iii}–Cu2–O7	169.31(6)
O7–Cu1–O1	87.20(6)	O7^{iii}–Cu2–O7	80.43(6)
N2^{ii}–Cu1–O1	89.15(6)	O6^{iii}–Cu2–N1	89.49(7)
O3^{i}–Cu1–O5	102.09(6)	O7^{iii}–Cu2–N1	169.15(6)
O7–Cu1–O5	92.42(6)	O7–Cu2–N1	97.53(6)

[a] Symmetry codes: (i) $1 - x$, $1/2 + y$, $-1/2 - z$; (ii) $2 - x$, $-1/2 + y$, $1/2 - z$; (iii) x, $1/2 - y$, $1/2 + z$. [b] Symmetry codes: (i) $1 - x$, $1 - y$, $-z$; (ii) $1/2 - x$, $1/2 + y$, $1/2 - z$; (iii) $1/2 - x$, $1/2 - y$, $-z$.

According to the concept of SBUs, this structure can be reduced to a schematic that rationalizes the structure as the assembly of $[Cu_2(CO_2)_2O_2N_4]$ SBUs, as shown in Figure 2 (c). Each SBU has eight vertices to eight adjacent SBUs. By treating the SBU as a single node and connecting the nodes according to the connectivity defined by nicotinate and isonicotinate ligands, a CsCl-like 3D network sustained by 8-connected nodes is formed, as illustrated in Figure 3. Although there is only one type of node in this net, there are two different links, identified by two different node–node distances (8.351 and 10.774 Å). The isonicotinate ligand defines the longer node–node distance and connects the nodes into a (4,4) 2D net, while the nicotinate ligand defines the shorter node–node distance and connects the nodes into another (4,4) 2D net parallel to the *bc* plane. These two types of nets intersect at an angle of 75.65° to generate the distorted CsCl net. To the best of our knowledge, this is the first transition metal complex with this unusual CsCl topology.

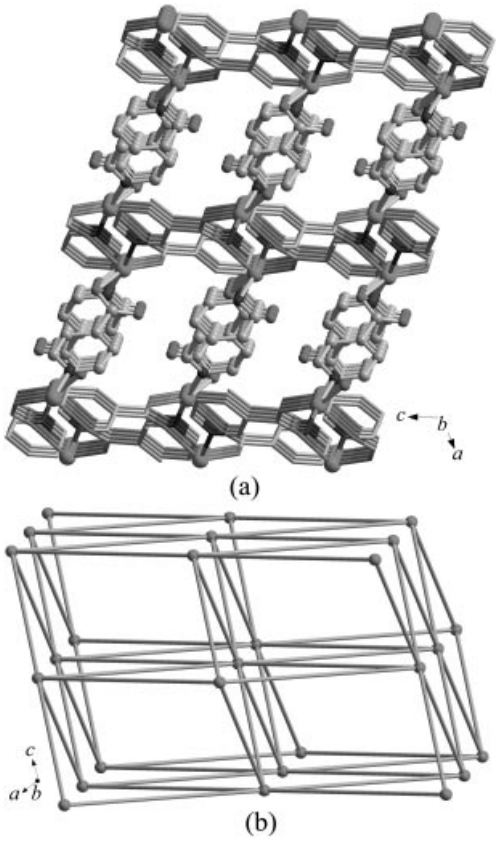

Figure 3. (a) The 3D packing structure of **1**; (b) schematic representation of the distorted CsCl net in complex **1**.

X-ray Crystal Structure of $[Cu_2(\mu_3\text{-OH})(isonicotinate)_2(BDC)_{0.5}]_n$ (2)

The single-crystal X-ray diffraction study showed that complex **2** consists of tetranuclear Cu^{II} clusters linked by isonicotinate and the BDC ligand. As shown in Figure 4, the tetranuclear cluster contains two independent Cu centres: one Cu centre (Cu1) has a distorted trigonal-bipy-

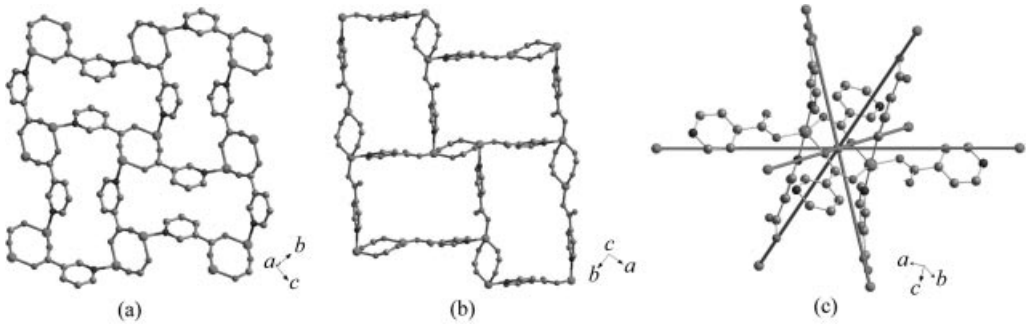

Figure 2. (a) View of the 2D (4,4) net constructed from dimetallic clusters and nicotinate ligands; (b) view of the 2D (4,4) net constructed from dimetallic clusters and isonicotinate ligands; (c) view of the 8-connected SBU in complex **1**, illustrating the connections to eight neighbours.

ramidal geometry and is bound by one BDC ligand, three different isonicotinate ligands and one hydroxide ion, whereas the other Cu centre (Cu2) has a distorted square-pyramidal geometry and is bound by one BDC ligand, two independent isonicotinate ligands and two hydroxide ions. A pair of CuO_4N square-pyramidal polyhedra share an edge with each other and a corner with two CuO_4N trigonal-bipyramidal polyhedra through two μ_3-hydroxy groups (Figure 5, e). The centre of inversion is situated in the middle of the two μ_3-hydroxy groups. The four copper ions, which lie on a plane, form an approximate parallelogram. Two μ_3-hydroxy groups bridge four Cu centres with an adjacent Cu···Cu separation in the range of 3.006 to 3.342 Å.

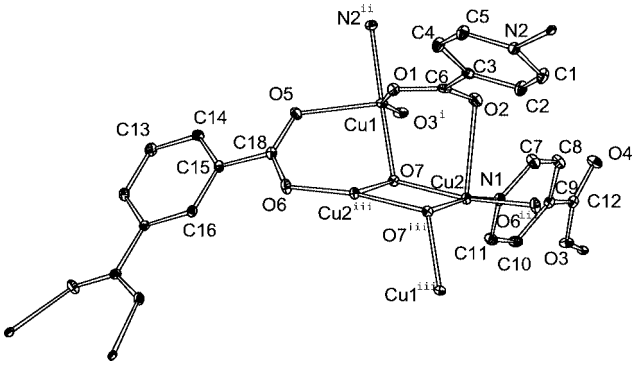

Figure 4. An ORTEP drawing of the molecular structure of complex **2**. For definition of i, ii and iii see footnote b in Table 1.

The asymmetric unit of **2** also contains two independent isonicotinate ligands, each of which has different coordination modes: one isonicotinate ligand acts as a μ_3-bridge and links the tetranuclear clusters to form a 2D sheet parallel to *bc* plane (Figure 5, a), while the other isonicotinate ligand binds through one O donor and one N donor to bridge the tetranuclear clusters and form a 1D double-chain (Figure 5, b). At the same time, the BDC ligand acts as a μ_4-bridge and links the tetranuclear clusters to form a 1D zigzag chain (Figure 5, c). In other words, each tetranuclear copper cluster binds to two BDC ligands and eight isonicotinate ligands simultaneously (Figure 5, d).

Four Cu polyhedra and four carboxylate carbon atoms represent a 10-connected inorganic SBU, as illustrated in Figure 5 (e). Although ten bridging ligands ligate each SBU, each SBU is connected to only eight nearest neighbours because two pairs of isonicotinate ligands form "double bridges". By treating the SBU as a single node and connecting the nodes according to the connectivity defined by the BDC and isonicotinate ligands (the double bridge being considered as one connection), a non-CsCl 3D network sustained by 8-connected nodes is then formed, as illustrated in Figure 6. This net is clearly different from other reported network topologies containing 8-connected nodes[5,6c] and adopts an unprecedented $3^5.4^{11}.5^8.6^4$ topology.[9] The asymmetric unit of **2** contains one BDC ligand and two independent isonicotinate ligands such that three different node–node distances (9.726, 10.362 and 10.940 Å) can be iden-

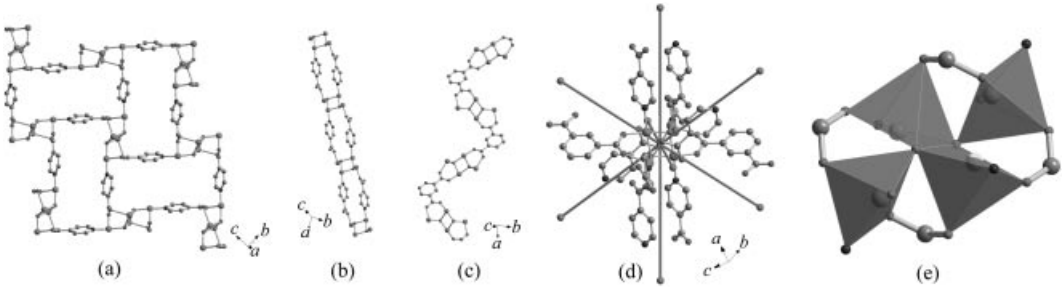

Figure 5. (a) View of the 2D (4,4) net constructed from tetranuclear clusters and isonicotinate ligands; (b) view of the 1D double-chain constructed from tetranuclear clusters and the second independent isonicotinate ligands; (c) view of the 1D zigzag chain constructed from tetranuclear clusters and BDC ligands; (d) view of the 10-connected SBU in complex **2**, illustrating the connections to eight neighbours; (e) view of the SBU in complex **2**, illustrating the four Cu polyhedra.

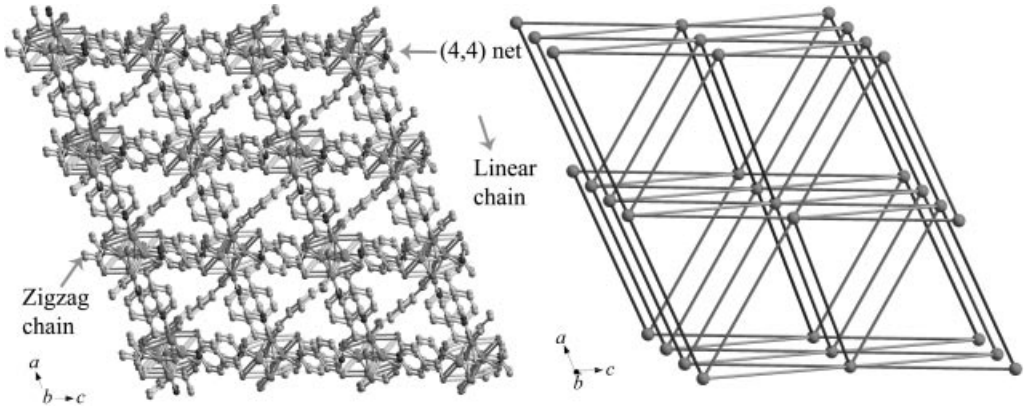

Figure 6. Left: the 3D packing structure of **2**; right: schematic representation of the $3^5.4^{11}.5^8.6^4$ topology in complex **2**.

tified. Each node, which is located at the symmetrical centre, links six neighbours in one plane, and the angles between the adjacent nodes are 54.251°, 65.904° and 59.845°, respectively.

The structure of **2** is completely different from the CsCl net and the other two previously known non-CsCl eight-connected nets. As shown in Figure 7, the parallel (4,4) nets of all nets are cross-linked by zigzag chains, although the detailed connection modes are different: in CsCl, the zigzag chain in the inter-layer region bridges the diagonal of a single window in the (4,4) net (Figure 7, a), in the $3^3 4^{15} 5^8 6^2$ topological net the zigzag chains bridge the edges of one (4,4) net and the diagonal of the next (Figure 7, b),[5b] and in the third net the zigzag chains bridge the diagonal of two neighbouring windows (Figure 7, c),[6c] whereas in **2** the zigzag chain is out of a plane and bridges two zigzag chains in two (4,4) nets, which, moreover, are alternately arranged on the two sides of the (4,4) net.

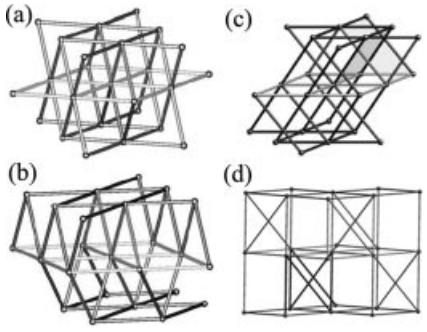

Figure 7. Difference between the four eight-connected nets: (a) CsCl-type net; (b) the $3^3 4^{15} 5^8 6^2$ topological net; (c) the self-penetrating eight-connected net; (d) the $3^5.4^{11}.5^8.6^4$ topology in complex **2**.

Magnetic Properties

The variable-temperature magnetic susceptibility of **1** was measured in the temperature range from 300 to 2 K (Figure 8), at a magnetic field strength of 5000 G. The $\chi_m T$ value at room temperature is 0.42 $cm^3 K mol^{-1}$, which is slightly bigger than the value of 0.375 $cm^3 K mol^{-1}$ expected for a noncoupled Cu^{II} ion with $g = 2$. Upon cooling, the $\chi_m T$ product decreases smoothly, thus indicating that a predominantly antiferromagnetic interaction exists in **1**. The $1/\chi_m$ vs. T (Curie) plot is linear. Fitting this curve to the Curie–Weiss law gives a Curie constant, C, of 0.454 $cm^3 K mol^{-1}$ and a Weiss constant, θ, of –18.13 K, which is a further indication of the weak antiferromagnetic interactions in **1**. According to the crystal structure of **1**, it can be assumed that the superexchange interactions between Cu^{II} ions through the bridging carboxylate groups are weak, which may lead to such a magnetic behaviour.

The Cu···Cu distance in **2**, which is much shorter than that in **1**, implies a weak Cu···Cu interaction. The variable-temperature magnetic susceptibility measurements of a powdered sample of complex **2** were performed in the temperature range 300–2 K. The magnetic behaviour of complex **2** is shown in Figure 9 in the form of $\chi_M T$ and χ_M^{-1} vs. T plots. The $\chi_M T$ value at room temperature is 1.50 $cm^3 K mol^{-1}$ per tetramer, which is consistent with the spin-only value for four uncoupled $S = 1/2$ centres with $g = 2$. Upon cooling, $\chi_M T$ decreases rapidly down to about 40 K, showing a dominant antiferromagnetic interaction between paramagnetic Cu^{II} ions. A Curie–Weiss fitting above 50 K give a Weiss constant of –90 K; this large negative value demonstrates a strong antiferromagnetic coupling. The pathway of antiferromagnetic interactions may be between the adjacent copper centres (Cu···Cu = 3.006 to 3.342 Å) bridged by a μ_3-hydroxy group. The decrease of $\chi_M T$ is less pronounced between 40 and 20 K, tending to a small plateau at a value (ca. 0.7 $cm^3 K mol^{-1}$) close to that expected for two uncoupled electrons resulting from an antiferromagnetically coupled tetranuclear Cu^{II} compound. Below 20 K, a rapid decrease appears due to further intra- and inter-tetramer antiferromagnetic interactions.

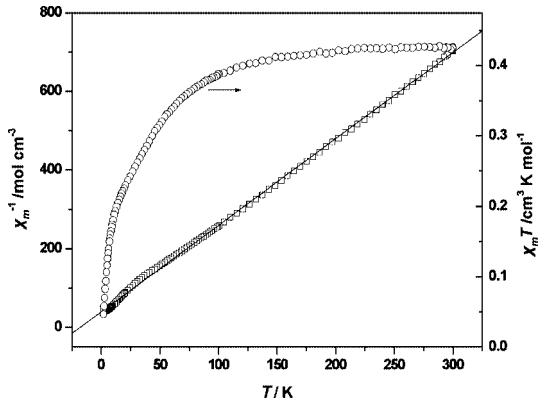

Figure 8. Plots of the temperature dependence (from 300 to 2 K) of $\chi_m T$ and χ_m^{-1} for **1**.

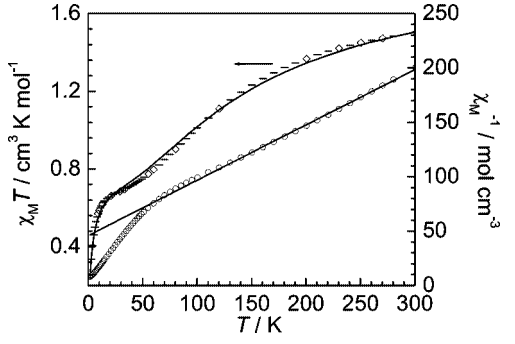

Figure 9. Plots of the temperature dependence (from 300 to 2 K) of $\chi_m T$ and χ_m^{-1} for **2**.

Considering the butterfly arrangement of the Cu^{II} ions in **2**, the experimental magnetic susceptibility data were analysed with the modified analytical expression derived by combining the tetramer model with $S = 1/2 \cdot [H = -J_1(S_1 + S_2)\cdot(S_3 + S_4) - J_2 S_3 \cdot S_4]$ by Murugavel[10] and inter-tetramer interactions (J) under the molecular-field approximation.[11] The best fitting for the experimental data gives $J_1 = -56.7\ cm^{-1}$, $J_2 = -114.9\ cm^{-1}$, $g = 2.25$ and $zj' =$

$-3.38\ cm^{-1}$. The agreement factor $R = \Sigma[(\chi_M T)_{obs} - (\chi_M T)_{calc}]^2/\Sigma(\chi_M T)_{obs}^2$ is 3.93×10^{-4}.

Conclusion

In summary, two 8-connected nets of a CsCl-type and an unusual $3^5.4^{11}.5^8.6^4$ topology have been structural characterised. The size of the SBUs increases from dinuclear to tetranuclear and their connections also increase from eight-connected to ten-connected. We have confirmed that SBUs can adopt highly connected nodes that can be employed for the construction of highly connected frameworks.

Experimental Section

General Remarks: All the syntheses were performed in Teflon-lined stainless-steel autoclaves under autogenous pressure. Reagents were purchased commercially and were used without further purification. Elemental C,N,H analyses were performed on an EA1110 CHNS-0 CE elemental analyzer. IR (KBr pellet) spectra were recorded with a Nicolet Magna 750FT-IR spectrometer. Variable-temperature magnetic susceptibilities in the temperature range 2–300 K were performed with a model CF-1 superconducting extracting sample magnetometer with the powdered sample kept in the capsule for weighing. All data were corrected for diamagnetism of the ligands estimated from Pascal's constants.

$[Cu(isonicotinate)(nicotinate)]_n$ (1): An aqueous mixture (15 mL) containing $CuNO_3{\cdot}3H_2O$ (0.24 g, 1 mmol), isonicotinic acid (0.123 g, 1 mmol) and nicotinic acid (0.123 g, 1 mmol) was placed in a Parr Teflon-lined stainless-steel bomb, which was sealed and placed in a programmable furnace. The temperature was raised to 160 °C over 4 h and held at that temperature for 60 h, then cooled over 60 h to 80 °C and finally cooled down to room temperature over 12 h. The resulting rectangular blue crystals were collected (0.1 g, 32.49% yield). This compound is stable in air and is insoluble in water and common organic solvents. $C_{12}H_8CuN_2O_4$ (307.74): calcd. C 46.91, H 2.63, N 9.12; found C 47.05, H 2.66, N 8.98. IR (solid KBr pellet): $\tilde{\nu}$ = 3434 (w), 3119 (s), 1651 (w), 1629 (vs), 1398 (vs), 1385 (s), 693 (w), 613 (w) cm^{-1}.

$[Cu_2(\mu_3\text{-}OH)(isonicotinate)_2(BDC)_{0.5}]_n$ (2): A mixture containing $Cu(OH)_2{\cdot}CuCO_3$ (0.44 g, 2 mmol), 1,3-benzenedicarboxylic acid (0.1 g, 0.6 mmol), isonicotinic acid (0.123 g, 1 mmol) and distilled water (10 mL) was placed in a Teflon-lined stainless-steel bomb, which was sealed and placed in a programmable furnace. The temperature was raised to 160 °C over 4 h and held at that temperature for 60 h, then cooled over 60 h to 80 °C and finally cooled down to room temperature over 12 h. The blue prismatic crystals were collected (0.1 g, 64% yield). This complex is stable in air and is insoluble in water and common organic solvents. $C_{16}H_{11}Cu_2N_2O_7$ (470.35): calcd. C 40.95, H 2.36, N 5.97; found C 41.05, H 2.66, N 5.98. IR (solid KBr pellet): $\tilde{\nu}$ = 3314 (w), 3108 (s), 1614 (s), 1559 (m), 1401 (vs), 1087 (m), 751 (m), 728 (m) cm^{-1}.

X-ray Crystallographic Study: X-ray intensities of complexes **1** and **2** were collected on a Siemens Smart CCD diffractometer equipped with a graphite-monochromated Mo-K_α radiation source (λ = 0.71073 Å) at 293(2) K. Empirical absorption corrections were applied to the data using the SADABS program.[7] The structures were solved by direct methods and refined by full-matrix least-squares on F^2 using the SHELXTL-97 program.[8] All of the non-hydrogen atoms were refined anisotropically. The H atoms bonded to C atoms were positioned geometrically and refined using a riding model. Crystallographic data and other pertinent information for **1** and **2** are summarised in Table 2. Selected bond lengths and angles are listed in Table 1.

Table 2. Crystallographic data for **1** and **2**.

	1	**2**
Empirical formula	$C_{12}H_8CuN_2O_4$	$C_{16}H_{11}Cu_2N_2O_7$
Temperature [K]	293(2)	293(2)
Crystal colour	blue	blue
Crystal size	$0.30 \times 0.25 \times 0.22$	$0.30 \times 0.08 \times 0.05$
Formula weight	307.74	470.35
Crystal system	monoclinic	monoclinic
Space group	$P2_1/c$	$C2_1/c$
a [Å]	9.5505(5)	17.922(2)
b [Å]	11.6346(4)	12.550(1)
c [Å]	11.9841(6)	16.492(2)
β [°]	113.083(2)	111.309(4)
V [Å^3]	1225.01(10)	3456.0(7)
Z	4	8
Density (calculated)	1.669	1.808
Abs. coeff. [mm^{-1}]	1.793	2.504
F(000)	620	1880
Reflections collections	3439	12983
Independent reflection	2143 [R(int) = 0.0405]	3927 [R(int) = 0.0194]
Goodness-of-fit on F^2	1.070	1.070
$R1$,$wR2$ [$I > 2\sigma(I)$]	0.0601, 0.1356	0.0259, 0.0597
$R1$,$wR2$ (all data)	0.0923, 0.1614	0.0298, 0.0616

CCDC-272139 (for **1**) and -272140 (for **2**) contain the supplementary crystallographic data for this paper. These data can be obtained free of charge from The Cambridge Crystallographic Data Centre via www.ccdc.cam.ac.uk/data_request/cif.

Acknowledgments

This work was supported by grants from the State Key Basic Research and Development Plan of China (001CB108906), the NNSF of China (nos. 29733090 and 20173063) and the NSF of Fujian Province (E0020001).

[1] For recent reviews, see for example: a) C. Janiak, *Dalton Trans.* **2003**, 2781–2804; b) B. Moulton, M. J. Zaworotko, *Chem. Rev.* **2001**, *101*, 1629–1658; c) L. Carlucci, G. Ciani, D. M. Proserpio, *Coord. Chem. Rev.* **2003**, *246*, 247–289.

[2] a) A. F. Wells, *Three-Dimensional Nets and Polyhedra*; Wiley-Interscience: New York, **1977**; b) A. F. Wells, *Further Studies of Three-Dimensional Nets*; ACA Monograph 8; American Crystallographic Association, **1979**.

[3] See for example: a) S. R. Batten, R. Robson, *Angew. Chem. Int. Ed.* **1998**, *37*, 1460–1494; b) O. M. Yaghi, M. O'Keeffe, N. W. Ockwig, H. K. Chae, M. Eddaoudi, J. Kim, *Nature* **2003**, *423*, 705–714; c) S. R. Batten, *CrystEngCommun* **2001**, *3*, 67–72; d) A. J. Blake, N. R. Champness, P. Hubberstey, W. S. Li, M. A. Withersby, M. Schröder, *Coord. Chem. Rev.* **1999**, *183*, 117–138; e) O. V. Dolomanov, D. B. Cordes, N. R. Champness, A. J. Blake, L. R. Hanton, G. B. Jameson, M. Schröder, C. Wilson, *Chem. Commun.* **2004**, 642–643; f) J. Zhang, Y. Kang, R.-B. Zhang, Z.-J. Li, J.-K. Cheng, Y.-G. Yao, *CrystEngCommun* **2005**, *7*, 177–178; g) J. Zhang, Z.-J. Li, Y. Kang, J. K. Cheng, Y.-G. Yao, *Inorg. Chem.* **2004**, *43*, 8085–8091.

[4] a) H. Li, M. Eddaoudi, M. O'Keeffe, O. M. Yaghi, *Nature* **1999**, *402*, 276–279; b) N. L. Rosi, J. Eckert, M. Eddaoudi, D. T. Vodak, J. Kim, M. O'Keeffe, O. M. Yaghi, *Science* **2003**, *300*, 1127–1129; c) M. Eddaoudi, D. B. Moler, H. Li, B. Chen,

T. M. Reineke, M. O'Keeffe, O. M. Yaghi, *Acc. Chem. Res.* **2001**, *34*, 319–330.

[5] a) D.-L. Long, A. J. Blake, N. R. Champness, C. Wilson, M. Schröder, *Angew. Chem. Int. Ed.* **2001**, *40*, 2443–2447; b) D.-L. Long, R. J. Hill, A. J. Blake, N. R. Champness, P. Hubberstey, D. M. Proserpio, C. Wilson, M. Schröder, *Angew. Chem. Int. Ed.* **2004**, *43*, 1851–1854; c) R. J. Hill, D.-L. Long, A. J. Blake, N. R. Champness, P. Hubberstey, M. Schröder, *Acc. Chem. Res.* **2005**, *38*, 335–348.

[6] a) X. M. Zhang, R. Q. Fang, H. S. Wu, *J. Am. Chem. Soc.* **2005**, *127*, 7670–7671; b) L. Pan, H. Liu, X. Lei, X. Huang, D. H. Olson, N. J. Turro, J. Li, *Angew. Chem. Int. Ed.* **2003**, *42*, 542–546; c) X.-L. Wang, C. Qin, E.-B. Wang, Z.-M. Su, L. Xu, S. R. Batten, *Chem. Commun.* **2005**, 4789–4790.

[7] *SADABS*, G. M. Sheldrick, University of Göttingen, Germany. **1996**.

[8] Siemens, *SHELXTL* (Version 5.05). Siemens Analytical X-ray Instruments Inc., Madison, Wisconsin, USA. **1994**.

[9] O. V. Dolomanov, A. J. Blake, N. R. Champness, M. Schröder, *J. Appl. Crystallogr.* **2003**, *36*, 1283–1284.

[10] R. Murugavel, M. Sathiyendiran, R. Pothiraja, M. G. Walawalkar, T. Mallah, E. Riviére, *Inorg. Chem.* **2004**, *43*, 945–953. (Note: a $1/kT$ term is missing in the $\chi_M T$ expression).

[11] R. L. Carlin, *Magnetochemistry*, Springer, Berlin, **1986**.

Received: October 12, 2005
Published Online: March 30, 2006

